

Experimental Verification of the Relativistic Fine-Structure Term of the Klein-Gordon Equation in Pionic Titanium Atoms

L. Delker, G. Dugan, and C. S. Wu

Columbia University, New York, New York 10027

and

D. C. Lu

Yale University, New Haven, Connecticut 06520

and

A. J. Caffrey, Y. T. Cheng, and Y. K. Lee

Johns Hopkins University, Baltimore, Maryland 21218

(Received 28 August 1978)

A newly designed, large-aperture and high-resolution bent-crystal spectrometer has been used to observe high-intensity sources of pionic x rays. The pionic x-ray source was a target of natural titanium which was placed adjacent to a copper pion-production target in the external beam of the Nevis synchrocyclotron. The energy difference between the $5g \rightarrow 4f$ and $5f \rightarrow 4d$ transitions in pionic titanium was measured to be 87.6 ± 1.8 eV. Comparison with the prediction of the Klein-Gordon equation is made.

High-resolution studies of pionic x rays using a bent-crystal spectrometer have in the past been limited by the low efficiency of the instrument and the lack of an adequately intense source.^{1,2} This deficiency can be effectively remedied by either a strong pion beam such as at a meson facility, or, as in the recent work of Marushenko *et al.*,³ by placing the x-ray target directly next to the pion-production target. In this latter approach, although the high resolution of the spectrometer has proven to be adequate in discerning the x rays from a very high background, the signal-to-background ratio is relatively low. In an experiment at the Nevis synchrocyclotron, we have modified the experimental approach used by Marushenko *et al.*³ By use of a 2- μ A extracted proton beam and a new target design, significant improvements in counting rate and signal-to-background ratio were achieved over previous attempts.^{3,4} A new technique of crystal bending was also used to achieve an improvement of fractional energy resolution ($\Delta E/E$) by a factor of 4 over that of Ref. 3. The combined experimental improvements enabled us to increase greatly the accuracies of the energy determinations of selected transitions [e.g., the π -Ti ($5g \rightarrow 4f$)], and also to observe the low-yield fine-structure component π -Ti ($5f \rightarrow 4d$), providing an experimental measurement of the relativistic fine-structure splitting in this pionic atom.

The experimental setup is shown in Fig. 1. A pion-production target, consisting of 32 separated sheets of Cu totaling 44.4 g/cm², was placed in the extracted beam. This pion target

was shielded from direct view of the spectrometer by a flat plug of brass and lead (see Fig. 1). The Ti x-ray target consisted of four slabs of natural titanium, mounted as shown in Fig. 1.

The bent crystal was located 6.4 m from the x-ray target, and had a focal length of 351 cm. About 1 m upstream from the crystal, a 91-cm-long tapered multislit collimator served as an additional background-suppression device. The bent crystal was an 11-cm by 11-cm slab of 1.4-mm-thick 310 quartz, housed in a temperature-regulated enclosure. The "intrinsic" angular resolution of the crystal (full width at half maximum) was measured to be 6.5 sec of arc. The diffracted radiation from the crystal was allowed to pass through a slit, set at 170 μ m wide, into a Ge detector assembly located inside a lead shielding box.

The detector assembly consisted of two hyperpure Ge crystals, each 5 mm by 5 mm by 6 cm, mounted one above the other to give a total height of 12 cm. Data from these two Ge detectors were collected, stored, and analyzed separately. The energy resolution of each Ge detector was 1 keV at 40 keV.

The spectrometer was enclosed in a cave to reduce the neutron background (see Fig. 1). To provide additional background reduction, the proton beam was extracted over a period of 20 μ sec rather than the usual 5 msec; the Ge detector pulses were gated off except during the proton beam spill, eliminating virtually all background not promptly produced by the proton beam.

The diffracted radiation was scanned by moving

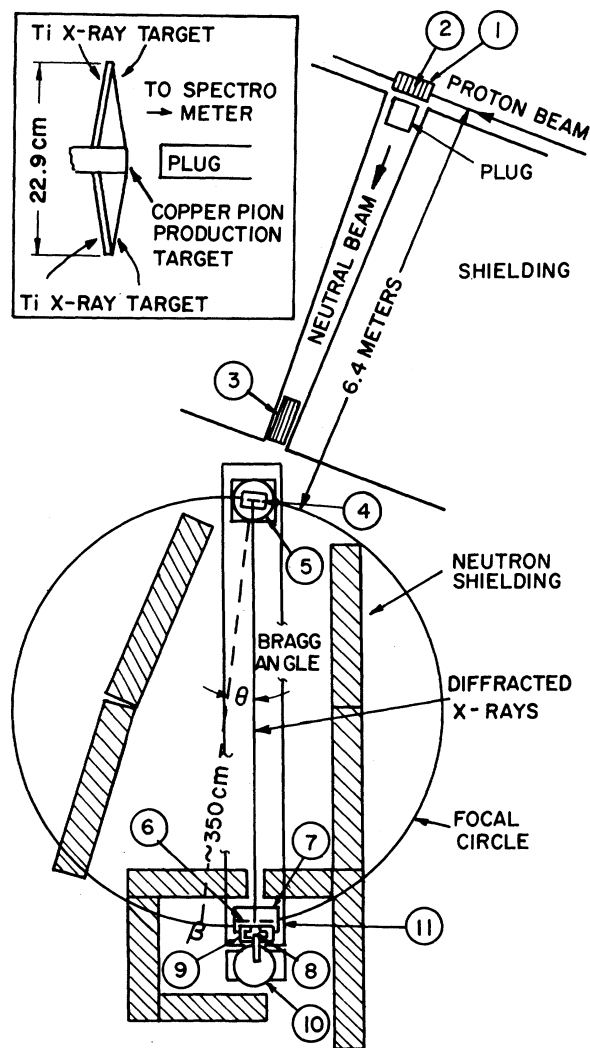


FIG. 1. Experimental layout of crystal spectrometer, collimator, and pion targets. Inset shows detail of pion production and x-ray targets. (1) X-ray target; (2) π^- production target; (3) collimator; (4) bent crystal; (5) turnable crystal mount; (6) thin slit; (7) slit table; (8) solid-state detector (Ge); (9) detector shield; (10) Dewar; (11) spectrometer frame.

the 170- μm slit across the angular range of interest over the focal plane with the crystal orientation fixed. The slit motion was remotely controlled by a computer, which also collected data from the Ge detectors. Data collection time at each slit position was determined by the number of protons on the production target, as measured by the integral of the proton current. In a typical 24-h run, the diffracted line was scanned thirty times, so that fluctuations in the line intensity due to small shifts in the position of the proton

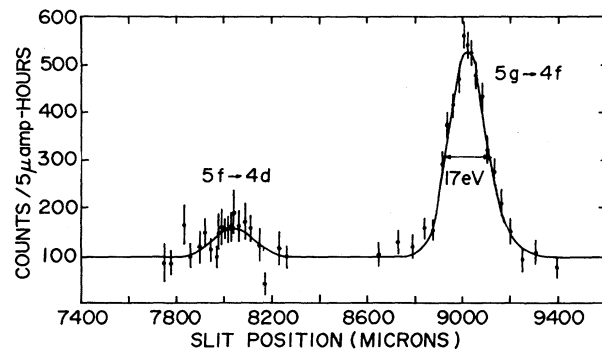


FIG. 2. Crystal spectrometer spectrum (with Ge background subtracted) of fine-structure components of the 5 \rightarrow 4 transition in pionic titanium. Solid line is best fit to the data, with a χ^2 of 28.7 for 35 degrees of freedom.

beam on target were averaged out.

The spectrometer line shape was calibrated with the 40.584-keV γ ray from a 1.5-Ci source of ^{99}Mo ,⁵ which had the same geometry as that of the pionic x-ray source. The instrumental line shape was determined to be an asymmetric Gaussian (a Gaussian with an exponential tail) integrated over the width of the transmission slit. The energy resolution of the spectrometer was measured to be 17 eV. The efficiency of the spectrometer at this energy was measured to be on the order of 0.5×10^{-9} . The energy scale of the spectrometer was calibrated using the $K\alpha_1$ x ray of Sm at 40.1181 keV,⁶ and the $K\alpha_2$ x ray of Eu at 40.9019 keV.⁶ Because these energies are used only to determine the energy scale, even relatively large ($\pm 0.1\%$) uncertainties or changes in these numbers contribute virtually no error to the final relative energy measurement reported below. These x rays were produced in fluorescent targets which had the same geometry as that of the pionic x-ray target. As a check of the stability of the spectrometer, the ^{99}Mo γ ray was calibrated before and after the measurement of the pionic Ti x rays, and the position of the line was found to be stable within 1.5 μm .

For each slit position, a pulse-height spectrum from the Ge detectors was obtained. Each of these spectra was fitted to a Gaussian line shape plus a linear background. This linear background was subtracted and the area of the Gaussian for each slit position was extracted. This procedure removes the ambient background appearing in the Ge detector spectrum and its fluctuations. The extracted areas, however, still contain a diffracted pionic x-ray signal. This is shown in

Fig. 2, where the areas of the Gaussians from the bottom Ge detector are plotted as a function of slit position for the $5g \rightarrow 4f$ and $5f \rightarrow 4d$ transitions in pionic titanium. The signal-to-background ratio for the $5g \rightarrow 4f$ transition, before the ambient background subtraction, was 0.75. The data for the $5f \rightarrow 4d$ transition correspond to $81 \mu\text{A} \cdot \text{h}$ of protons on target.

The crystal spectrometer spectrum shown in Fig. 2 has been fitted assuming two peaks and a linear background. With the inclusion of small hyperfine effects due to the isotopes of natural titanium,⁷ the linewidths of each transition, which are assumed to be equal, are consistent with the instrumental resolution. (The strong-interaction width of the $5f \rightarrow 4d$ transition has been estimated to be less than 1 eV and has been neglected.) Using the data from both the top and bottom detectors, we find an intensity ratio of $(16.4 \pm 3.4)\%$ and a separation energy of 87.6 ± 1.8 eV between the $5f \rightarrow 4d$ and $5g \rightarrow 4f$ transitions.

The observed separation energy can be compared with the predicted fine structure. The major part of this separation for the $5f \rightarrow 4d$ and $5g \rightarrow 4f$ transitions is due to the relativistic fine-structure splitting predicted by the Klein-Gordon equation for the Coulomb potential from a point nucleus. This is modified by corrections from vacuum polarization, electron screening, and the strong interaction between the pion and the nucleus. These contributions are listed in Table I. The vacuum polarization is calculated in perturbation theory.⁸ To account for the uncertainty in electron screening due to the competition between preceding Auger transitions and subsequent refilling, we give our estimate based on 1 ± 1 K electron only. The strong-interaction shift is calculated in perturbation theory, using a pion-nucleus optical potential⁹ with parameters given by Tauscher.¹⁰ The uncertainty from the strong interaction, which is the largest theoretical uncertainty, is taken to be ± 1 eV, based on the variations in the shift obtained by using different

sets of potential parameters obtained from other pionic-atom data.¹¹ The final calculated energy difference, 88.1 ± 1.2 eV, is in good agreement with the measured energy splitting.

Although the agreement between the calculations and the experimental measurement does verify the predictions of the Klein-Gordon equation in lowest order, it does not distinguish between that equation and the Schrödinger equation with relativistic corrections. This is because the prediction of the Klein-Gordon equation for the relativistic fine-structure splitting is the same, to first order in $(\alpha Z/n)^2$, as the splitting one would calculate in perturbation theory resulting from the relativistic corrections to the Schrödinger equation. The experimental uncertainties are considerably larger than higher-order terms in $(\alpha Z/n)^2$.

Noncircular transitions predicted by the Klein-Gordon equation have been previously observed with Ge detectors.¹² In the recent work of Carter *et al.*¹² eight cases of noncircular transitions were observed of which three cases are relatively free from strong-interaction effect and relevant to the test of the Klein-Gordon equation. The agreement with the predictions is good. However, in this previous work, the splittings were not completely resolved; also, the details of the determinations of the splittings were not described in the paper. The term of order $mc^2(\alpha Z/n)^4$ in the Klein-Gordon-equation energy eigenvalue, which is partly responsible for the level splittings, can also be tested at the level of 2% or better from absolute energies of x rays from transitions between circular orbits in high- Z pionic atoms (with a precision of about 50 ppm), provided that the pion mass is known independently (i.e., not from pionic x-ray measurements) with the same relative precision. However, this is an indirect measurement of the relativistic term; the virtue of the fine-structure splitting measurement made in this work is that it is a direct confirmation of this term performed by

TABLE I. Calculated energy differences, $E(5f \rightarrow 4d) - E(5g \rightarrow 4f)$, in pionic titanium (in eV).

Klein-Gordon equation, point-nucleus Coulomb potential	59.3
Vacuum polarization, first order $[\alpha(Z\alpha)]$	25.2
Vacuum polarization, higher orders $[\alpha^2(Z\alpha), \alpha(Z\alpha)^3, 5, 7]$	0.4
Electron screening, 1 ± 1 ls electrons	-0.6 ± 0.6
Strong interaction	3.8 ± 1.0
Total calculated energy difference	88.1 ± 1.2

relative energy measurements, independent of precise knowledge of the pion mass.

We are grateful for help by the Nevis synchrotron staff members throughout this experiment, and by Dr. M. Holland, Dr. S. Cheng, and Dr. D. Stromswald in beam construction at the initial stage of the experiment. This research was supported in part by the National Science Foundation and the U. S. Department of Energy.

¹A. Astbury *et al.*, in *Congrès International de Physique Nucléaire* (Dunod, Paris, 1964), Vol. II, p. 225.

²R. E. Shaefer, *Phys. Rev.* **163**, 1451 (1967).

³V. N. Marushenko *et al.*, *Pis'ma. Zh. Eksp. Teor. Fiz.* **23**, 80 (1976) [*JETP Lett.* **23**, 72 (1976)].

⁴F. Boehm *et al.*, *Phys. Rev. Lett.* **38**, 215 (1977).

⁵C. W. E. van Eijk *et al.*, *Nucl. Phys.* **A121**, 440

(1968).

⁶J. A. Bearden, *Rev. Mod. Phys.* **39**, 78 (1967).

⁷C. M. Lederer, J. M. Hollander, and I. Perlman, *Table of the Isotopes*, edited by C. M. Lederer *et al.* (Wiley-Interscience, New York, 1967), pp. 180-183.

⁸J. Blomqvist, *Nucl. Phys.* **B48**, 95 (1972).

⁹M. Ericson and T. E. O. Ericson, *Ann. Phys. (N.Y.)* **36**, 323 (1966).

¹⁰L. Tauscher, in *Proceedings of the International Seminar on the π -Meson Nucleus Interaction*, Strasbourg, 1971 (unpublished).

¹¹D. A. Jenkins and R. Kunselman, *Phys. Rev. Lett.* **17**, 1148 (1966); G. Backenstoss, *Annu. Rev. Nucl. Sci.* **20**, 501 (1970); R. J. Powers, in *Meson-Nuclear Physics—1976*, AIP Conference Proceedings No. 33, edited by P. D. Barnes, R. A. Eisenstein, and L. S. Kisslinger (American Institute of Physics, New York, 1976), p. 552; M. Leon, LAMPF Report No. LA-UR-77-1648, 1978 (to be published).

¹²A. L. Carter *et al.*, *Phys. Rev. Lett.* **37**, 1380 (1976).

Proposed Free-Electron Laser Stimulated by Traveling Microwave Radiation

Y. W. Chan

Department of Physics, The Chinese University of Hong Kong, Hong Kong

(Received 15 November 1978)

A free-electron laser excited by traveling microwave radiation is suggested and discussed. Some desirable features of the microwave free-electron laser are given.

Recently, the first operation of a free-electron laser was reported by Deacon *et al.*,¹ soon after the stimulated emission of radiation by relativistic electrons in a spatially periodic transverse magnetic field had been successfully observed by Elisa *et al.*² The apparatus of this laser consists of a superconducting double helix to produce a transverse and circularly polarized periodic static magnetic field of 2.4 kG, a beam of 43-MeV electron bunches traveling along the axis of the helix to interact with the periodic magnetic field, and a pair of mirrors located at the ends of the interaction region to provide feedback. The stimulated emission of bremsstrahlung in a spatially periodic magnetic field, on the basis of which this magnetic free-electron laser was constructed and tested, was first analyzed by Madey³ and Madey, Schwettman, and Fairbank.⁴ However, some authors have subsequently shown,⁵⁻⁸ and also it is now known,⁹ that magnetic free-electron lasers are purely classical devices.

If the periodic static magnetic field in the apparatus is replaced by a traveling microwave as

the source of excitation, the apparatus becomes a microwave free-electron laser. Since microwave radiation is coherent, when a bunch of electrons is backscattered (antiparallel scattered) by a microwave, the electrons will be stimulated to oscillate coherently and to emit coherent radiation in the direction of the electron beam with a shorter wavelength and a higher intensity than that of the microwave, depending on the electron velocity and the number of electrons in each bunch. The physical process of the interaction is basically a Compton type of scattering. The microwave free-electron laser has some desirable features which deserve to be considered and studied. For examples: (1) A large scattering cross section is available in the backscattering process. (2) The wavelength of the stimulated radiation can be easily varied by varying the wavelength of the microwaves without changing the velocity of the electron beam. Hence the microwave method will provide extra tuning convenience. (3) The wavelength and the wave shape in each period of a microwave can be maintained more uniformly than that of a periodic